



Mesonic Resonance Production in p–Pb, Pb–Pb and Xe–Xe Collisions with ALICE at the LHC [†]

Dukhishyam Mallick, for the ALICE Collaboration

School of Physical Sciences, National Institute of Science Education and Research, HBNI, Jatni 752050, India; mallick.dukhishyam@cern.ch

[†] Presented at Hot Quarks 2018—Workshop for Young Scientists on the Physics of Ultrarelativistic Nucleus-Nucleus Collisions, Texel, The Netherlands, 7–14 September 2018.

Published: 15 April 2019



Abstract: We report recent measurements of mesonic resonance production in pp, p–Pb, Pb–Pb and Xe–Xe collision systems with the ALICE detector at LHC energies. Integrated particle yields, mean transverse momenta and particles ratios of mesonic resonances like $\rho(770)^0$, $K^*(892)^0$ and $\phi(1020)$ as a function of the charged particle multiplicity are presented. These measurements allow us to have better understanding of properties of the hadronic medium and hadrochemistry of the particle production from large (Pb–Pb and Xe–Xe) to small systems (pp, p–Pb). The flavour dependence of parton energy loss is also studied by measuring the nuclear modification factor, R_{AA} in Pb–Pb at $\sqrt{s_{NN}} = 2.76$ and 5.02 TeV and Xe–Xe at $\sqrt{s_{NN}} = 5.44$ TeV collisions.

Keywords: hadronic phase; hadrochemistry; flavour dependence

1. Introduction

Resonances are short lived particle having lifetimes $\sim 10^{-23}$ s. Due to their short lifetimes, they are useful tools to understand the mechanisms of particle production and properties of the hadronic phase formed in heavy-ion collisions. If the time interval between the chemical and kinetic freezeouts is comparable with the lifetime of the resonance, the hadronic phase has enough time for scattering of the daughter particles. As a result, the yield of resonances might be modified due to in-medium effects [1]. So, measurements of various resonances with lifetimes from ~ 1 fm/c to ~ 50 fm/c enable us to investigate the role of the re-scattering and regeneration processes in the hadronic medium. The nuclear modification factors (R_{AA}) of resonances along with other hadrons are used to study the energy loss of partons in the hot and dense medium [2].

In this proceedings, we present results on particle yield, mean transverse momentum $\langle p_T \rangle$, particle yield ratios and nuclear modification factor of $K^*(892)^0$ and $\phi(1020)$ production in p–Pb, Pb–Pb and Xe–Xe collisions at LHC energies. In addition, measurements of $\rho(770)^0$ meson production in pp and Pb–Pb collisions at $\sqrt{s_{NN}} = 2.76$ TeV are also discussed [3]. In the following $\rho(770)^0$, $K^*(892)^0$ and $\phi(1020)$ will be denoted as ρ , K^{*0} and ϕ , respectively.

2. Analysis Details

The measurements of K^{*0} and ϕ meson production have been performed in p–Pb collisions as a function of the event multiplicity at $\sqrt{s_{NN}} = 8.16$ TeV in the rapidity range $0.0 < y_{cm} < 0.5$. Similar measurements are also done at mid-rapidity ($|y| < 0.5$) for Xe–Xe collisions at $\sqrt{s_{NN}} = 5.44$ TeV and

Pb–Pb collisions at $\sqrt{s_{NN}} = 5.02$ TeV along with ρ meson production in pp and Pb–Pb collisions at $\sqrt{s_{NN}} = 2.76$ TeV.

The resonances are reconstructed by invariant mass of their decay daughters [2]. The K^{*0} , ϕ [4] and ρ [3] mesons are reconstructed through their hadronic channels $K^{*0}(\bar{K}^{*0}) \rightarrow K^+ \pi^- (K^- \pi^+)$ (BR = 66.6%), $\phi \rightarrow K^+ K^-$ (48.2 %) and $\rho \rightarrow \pi^+ \pi^-$ (100 %), respectively [5]. Particle identification (PID) is performed using the Time Projection Chamber (TPC) and the Time of Flight (TOF) detector. PID in TPC is based on the specific energy loss (dE/dx) of each particle in the TPC gas and particles are identified by their time of flight with TOF. The forward detector V0, which consists of two sub-detectors V0-A and V0-C, is used for triggering and measurement of event multiplicity/centrality classes [6]. The invariant mass distribution of unlike charged daughter pairs from same event contains the resonance signal along with a large combinatorial background. The combinatorial background is estimated by using mixed event and like-sign techniques. In the event mixing technique, the opposite charged pairs of the decay daughters from the two mixed events must have similar characteristics such as multiplicity/centrality, collision vertex position etc. In like sign technique, the background is evaluated by using the invariant mass distribution of like-charge pairs from the same event [2]. After the combinatorial background is subtracted, the raw yields are obtained by integrating the signal distribution and then corrected for detector acceptance, tracking efficiency and branching ratio. The first two corrections are determined from Monte Carlo simulations of the ALICE detector response [7].

3. Results

Figure 1 (left panel) shows the integrated yields of K^{*0} normalised to the average charged particle multiplicity density ($\langle dN_{ch}/d\eta \rangle$) as a function of $\langle dN_{ch}/d\eta \rangle$ in pp collisions at $\sqrt{s} = 7, 13$ TeV and in p–Pb collisions at $\sqrt{s_{NN}} = 5.02, 8.16$ TeV. The scaled integrated yield is almost constant as a function of $\langle dN_{ch}/d\eta \rangle$, and the scaled integrated yields in different collision systems and at different energies are consistent within the uncertainties for similar multiplicities. This indicates that particle production is mainly driven by charged particle multiplicity irrespective of collision systems and energies. The right panel of Figure 1 shows the mean transverse momentum ($\langle p_T \rangle$) of K^{*0} as a function of the averaged charged particle multiplicity measured in pp collisions at $\sqrt{s} = 7, 13$ TeV and in p–Pb collisions (at $\sqrt{s_{NN}} = 5.02, 8.16$ TeV). $\langle p_T \rangle$ increases with increasing charged particle multiplicity and seems to saturate for high multiplicity p–Pb collisions. A similar trend in $\langle p_T \rangle$ as a function of charged particle multiplicity is also observed for other resonances [4]. The charged particle multiplicity in the most central p–Pb collisions have similar order of magnitude as peripheral heavy ion collisions [8]. The new results of $\langle p_T \rangle$ may lead to a better understanding of mass ordering (particles with similar masses have similar $\langle p_T \rangle$) which is observed in central and semi-central Pb–Pb collisions as expected from the hydrodynamic expansion of the system [2]. It breaks down in small collisions systems [7].

The ratio of p_T integrated particle yields as a function of $\langle dN_{ch}/d\eta \rangle^{1/3}$ for various resonances in different collision systems and energies measured with the ALICE detector are shown in Figure 2. The decreasing trends in the $\rho/\pi, K^{*0}/K, \Lambda(1520)/\Lambda$ ratios have been observed with increasing charged particle multiplicity. These results suggest dominance of re-scattering over regeneration in the hadronic phase for short lived resonances, ρ, K^{*0} , and $\Lambda(1520)$. On the other hand the ratios $\Sigma^{*\pm}/\Lambda, \Xi^{*0}/\Xi$ and ϕ/K are nearly constant across all systems and centrality classes and are not affected much by the hadronic phase. The measurements of these particle ratios are also compared with the EPOS model (with and without UrQMD) [9], represented as lines in the plot. The EPOS model with UrQMD switched on qualitatively describes the trend of the experimental data.

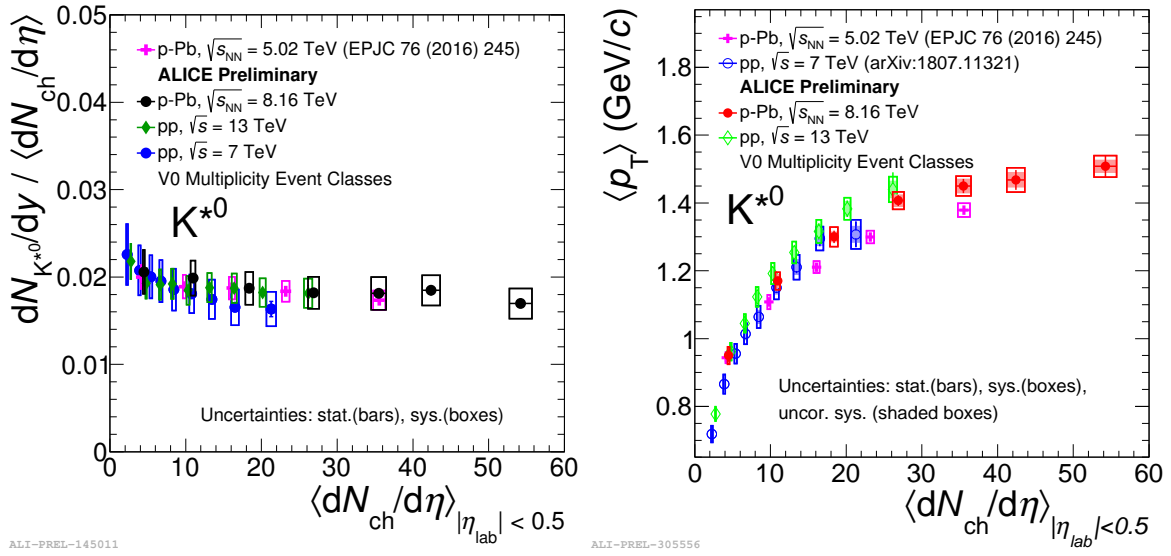


Figure 1. (Color online) Left panel: The integrated yields of K^{*0} normalised to $\langle dN_{ch}/d\eta \rangle$ in pp collisions at $\sqrt{s} = 7, 13$ TeV and in p–Pb collisions at $\sqrt{s_{NN}} = 5.02, 8.16$ TeV as a function of $\langle dN_{ch}/d\eta \rangle$. Right panel: Mean transverse momentum ($\langle p_T \rangle$) of K^{*0} as a function of $\langle dN_{ch}/d\eta \rangle$ in pp collisions at $\sqrt{s} = 7, 13$ TeV and in p–Pb collisions at $\sqrt{s_{NN}} = 5.02, 8.16$ TeV. Statistical uncertainties (bars) are shown together with total (hollow boxes) and multiplicity-uncorrelated (shaded boxes) systematic uncertainties.

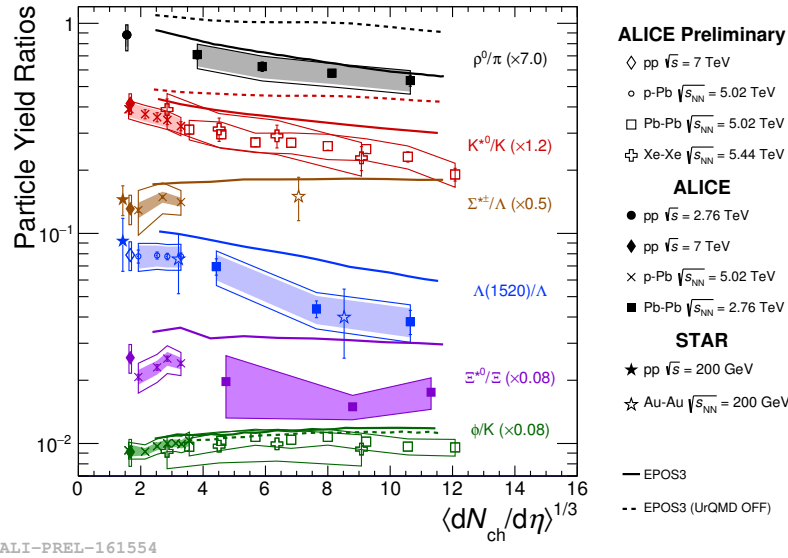


Figure 2. (Color online) p_T integrated particle yield ratios ρ/π , K^0/K , $\Lambda(1520)/\Lambda$, Σ^{*0}/Σ , Ξ^{*0}/Ξ and ϕ/K as a function of $\langle dN_{ch}/d\eta \rangle^{1/3}$ in pp, p–Pb, Pb–Pb and Xe–Xe collisions. The model predictions from EPOS3 (with and without URQMD) are also shown.

Figure 3 (left panel) shows the nuclear modification factor, R_{AA} of light flavor particles such as π , K , p , K^{*0} and ϕ as a function of p_T in Pb–Pb collisions at $\sqrt{s_{NN}} = 5.02$ TeV for centrality class 0–10%. At low p_T (< 2 GeV/c), the K^{*0} R_{AA} is smaller than R_{AA} of ϕ and charged hadrons [2]. In the intermediate p_T range (2–8 GeV/c), the baryon and meson R_{AA} values have different behaviour. At high p_T (> 8 GeV/c) all light flavour hadrons have similar R_{AA} values within uncertainties, this suggests no flavour dependence of R_{AA} at high p_T . The right panel of Figure 3 shows R_{AA} of K^{*0} in Xe–Xe collisions at $\sqrt{s_{NN}} = 5.44$ TeV and in

Pb–Pb collisions at $\sqrt{s_{NN}} = 5.02$ TeV for centrality classes with similar multiplicities. The result shows no significant system size dependence of R_{AA} .

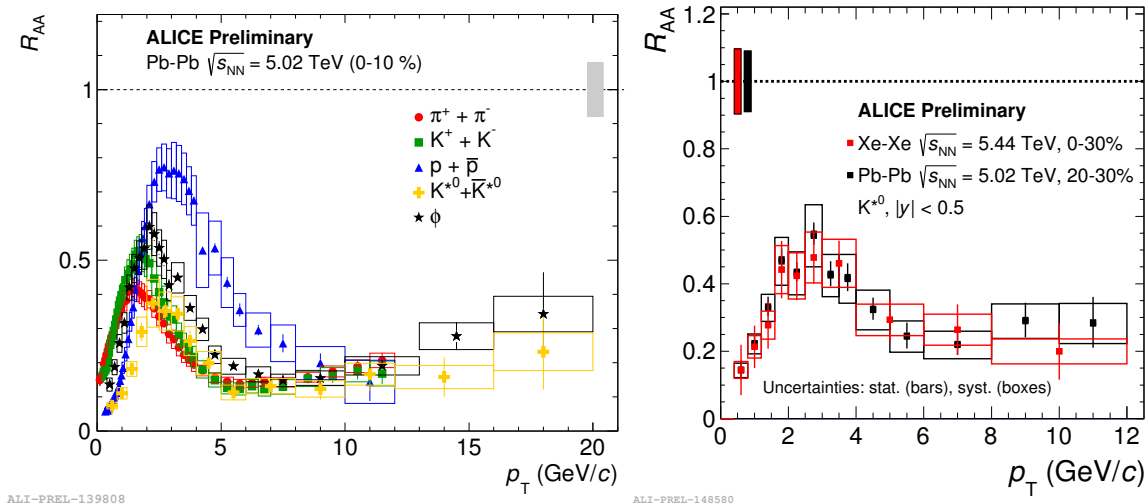


Figure 3. (Color online) Left panel: R_{AA} as a function of p_T of π , K , p , K^{*0} and ϕ for centrality class 0–10 % in Pb–Pb collisions at $\sqrt{s_{NN}} = 5.02$ TeV. Right panel: R_{AA} as a function of p_T of K^{*0} in Xe–Xe collisions at $\sqrt{s_{NN}} = 5.44$ TeV and Pb–Pb collisions at $\sqrt{s_{NN}} = 5.02$ TeV for centrality classes with similar charged particle multiplicity. The bars and the boxes represent the statistical and systematic uncertainties respectively. The boxes around unity indicate the uncertainty on the normalization of R_{AA} , including the uncertainty on the nuclear overlap function $\langle T_{AA} \rangle$ and the normalization uncertainty [2].

4. Summary

In summary, we have shown the results for K^{*0} and ϕ resonance production with the ALICE detector in p–Pb, Pb–Pb and Xe–Xe collisions at the LHC energies. The results include the recent measurements in p–Pb collisions at $\sqrt{s_{NN}} = 8.16$ TeV and Xe–Xe collisions at $\sqrt{s_{NN}} = 5.44$ TeV for various centrality/multiplicity classes. The $\langle p_T \rangle$ increases with increasing multiplicity and seems to saturate for high multiplicity in p–Pb systems. The p_T integrated yields of K^{*0} scaled by the average charged particle multiplicity are observed to be constant as a function of charged particle multiplicity density. This suggests that the event multiplicity drives the particle production irrespective of collision systems and energies. Ratio of p_T integrated yields shows a suppression with increasing multiplicity for short lived resonances, which suggests that re-scattering is a dominant process over regeneration for these resonances in the hadronic phase. For light flavoured hadrons, the R_{AA} shows no flavour dependence at high p_T (>8 GeV/c) within uncertainties. This points out the fact that the fragmentation in vacuum may be the dominant particle production mechanism in this kinematic regime [2]. For similar multiplicity classes, no significant system size dependence in the R_{AA} measurement is observed.

References

1. Abelev, B.; Adam, J.; Adamová, D.; Aggarwal, M.M.; Agnello, M.; Agostinelli, A.; Agrawal, N.; Ahammed, Z.; Ahmad, N.; Ahmad Masoodi, A.; et al. $K^*(892)^0$ and $\phi(1020)$ production in Pb–Pb collisions at $\sqrt{s_{NN}} = 2.76$ TeV. *Phys. Rev. C* **2015**, *91*, 024609, doi:10.1103/PhysRevC.91.024609.
2. Adam, J.; Adamová, D.; Aggarwal, M.M.; Aglieri Rinella, G.; Agnello, M.; Agrawal, N.; Ahammed, Z.; Ahmad, S.; Ahn, S.U.; Aiola, S.; et al. $K^*(892)^0$ and $\phi(1020)$ meson production at high transverse momentum in pp and Pb–Pb collisions at $\sqrt{s_{NN}} = 2.76$ TeV. *Phys. Rev. C* **2017**, *95*, 064606, doi:10.1103/PhysRevC.95.064606.

3. ALICE Collaboration. Production of the $\rho(770)^0$ meson in pp and Pb-Pb collisions at $\sqrt{s_{NN}} = 2.76$ TeV. *arXiv* **2018**, arXiv:1805.04365.
4. Adam, J.; Adamová, D.; Aggarwal, M.M.; Aglieri Rinella, G.; Agnello, M.; Agrawal, N.; Ahammed, Z.; Ahmad, S.; Ahn, S.U.; Aiola, S.; et al. Production of $K^*(892)^0$ and $\phi(1020)$ production in p-Pb collisions at $\sqrt{s_{NN}} = 2.76$ TeV. *Eur. Phys. J. C* **2016**, *76*, 245, doi:10.1140/epjc/s10052-016-4088-7.
5. Olive, K.A. Review of Particle Physics. *Chin. Phys. C* **2014**, *38*, 090001.
6. Abelev, B. Performance of the ALICE Experiment at the CERN LHC. *Int. J. Mod. Phys.* **2014**, *A29*, 1430044.
7. Dash, A.K. Multiplicity dependence of strangeness and hadronic resonance production in pp and p-Pb collisions with ALICE at the LHC. *arXiv* **2018**, arXiv:1807.07469. doi:10.1016/j.nuclphysa.2018.11.011.
8. Kim, B. ALICE results on system-size dependence of charged-particle multiplicity density in p-Pb, Pb-Pb and Xe-Xe collisions. *arXiv* **2018**, arXiv:1807.09061, doi:10.1016/j.nuclphysa.2018.09.060.
9. Knospe, A.G.; Markert, C.; Werner, K.; Steinheimer, J.; Bleicher, M. Hadronic resonance production and interaction in partonic and hadronic matter in the EPOS3 model with and without the hadronic afterburner UrQMD. *Phys. Rev. C* **2016**, *93*, 014911, doi:10.1103/PhysRevC.93.014911.



© 2019 by the authors. Licensee MDPI, Basel, Switzerland. This article is an open access article distributed under the terms and conditions of the Creative Commons Attribution (CC BY) license (<http://creativecommons.org/licenses/by/4.0/>).